

# Surface- and Bulk-Modified Galactoglucomannan Hemicellulose Films and Film Laminates for Versatile Oxygen Barriers

Jonas Hartman, Ann-Christine Albertsson,\* and John Sjöberg

Fibre and Polymer Technology, School of Chemical Science and Engineering, Royal Institute of Technology (KTH), Teknikringen 56-58, SE-100 44 Stockholm, Sweden

Received February 10, 2006; Revised Manuscript Received March 29, 2006

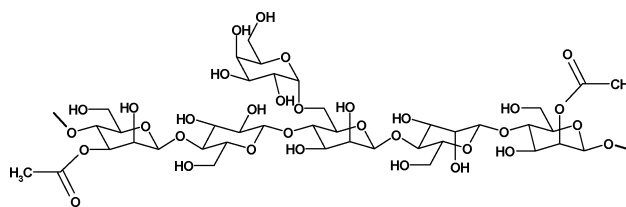
The objective of this study was to create oxygen barrier films based on the hemicellulose *O*-acetylgalactoglucomannan (AcGGM) that show high resistance toward moisture-rich conditions. We have applied Williamson benzylation, a classic derivatization method of carbohydrates, as well as two different methods for surface grafting, and, finally, lamination of unmodified hemicellulose films with the synthesized hydrophobic benzylgalactoglucomannan (BnGGM). It was found that the thermoplastically behaving BnGGM could form independent transparent and strong films that were easy to handle. As expected, their resistance toward water was very high, and the oxygen barrier properties showed drastically lower sensitivity toward moisture than films from the corresponding unmodified material. The surface grafting and lamination methods were approached in order to try and combine excellent barrier properties with moisture tolerance. It was found that the grafting methods applied had a positive effect in this direction; however, lamination turned out to be an even more promising option.

## 1. Introduction

The desire to widen the scope of the use of natural polymers, such as polysaccharides, is augmenting rapidly in times when renewable resources are needed more than ever. Chemical modification of polysaccharides has been exercised for more than a century with work focusing mostly on cellulose and starch. The plentiful number of hydroxyl groups gives excellent possibilities to property changes by substitution reactions. Basically, there are four main categories of substitutions; esterification, etherification, deoxyhalogenation, and acetalation. Established functionalized celluloses include cellulose nitrate, which is among the first polymeric materials used as a plastic, as such cellulose acetate, an important cellulose ester that is used for textile fibers and cigarette filters among other things, and carboxymethyl cellulose (CMC), a water-soluble ether derivative which has found widespread applications. Other cellulose ethers include benzyl cellulose, on which investigations started in 1917.<sup>1</sup> Benzylation of cellulose was initially performed to manufacture a useful thermoplastic cellulose derivative that could compete with plastized cellulose nitrate (i.e., celluloid) in order to broaden the area of application of cellulose material.<sup>2–5</sup> Today, benzyl cellulose can only be found in certain special applications such as filtration membranes.<sup>6</sup>

Related to cellulose, there are also hemicelluloses, such as *O*-acetylgalactoglucomannan (AcGGM, Scheme 1), having a main chain consisting of  $\beta$ -(1 $\rightarrow$ 4)-linked D-mannose and D-glucose with  $\alpha$ -(1 $\rightarrow$ 6)-linked D-galactose moieties in various amounts.<sup>7</sup> A difference is that these often form low-viscosity solutions in water due to substituents and low molar mass (generally less than 100 monosaccharide units). In a recent paper, we presented evidence that shows that AcGGM is promising as an oxygen barrier material but also that it is rather sensitive toward a high-moisture atmosphere, as expected (loss of barrier at higher humidities).<sup>8</sup> Lately, benzylations of the related materials xylan and konjac glucomannan have been done

**Scheme 1.** Structural Element of *O*-Acetylgalactoglucomannan (AcGGM)



for other purposes.<sup>9–12</sup> We thought that the small, strongly hydrophobic, and easily detectable benzyl group also would be a good selection for our specific goal to achieve versatile barrier films.

The aim of this paper was to produce oxygen barrier films exhibiting low moisture sensitivity through modification of the wood-derived hemicellulose *O*-acetylgalactoglucomannan (AcGGM). We report on the novel hydrophobic softwood galactoglucomannan derivative principally made by Williamson benzylation and its film properties in terms of water tolerance and oxygen permeability. Moreover, styrene grafting of films based on unmodified AcGGM by plasma and vapor-phase treatments have been performed. Finally, lamination of an unmodified AcGGM film with benzylated AcGGM was also investigated.

The benzylated AcGGM was analyzed by nuclear magnetic resonance (NMR), matrix-assisted laser desorption/ionization time-of-flight mass spectrometry (MALDI-TOF MS), attenuated total reflectance Fourier transform infrared spectroscopy (ATR-FTIR), and differential scanning calorimetry (DSC). The cast films were evaluated by contact angle measurement, infrared spectroscopy, dynamical mechanical analysis (DMA), and oxygen permeability measurement using Ox-Tran Mocon.

## 2. Experimental Section

**2.1. Materials.** *O*-Acetylgalactoglucomannan hemicellulose isolate was obtained from thermomechanical pulping (TMP) process water. The isolation method was based on ultrafiltration (UF) using hydrophilic

\* To whom correspondence should be addressed. Telephone: +46 8 790 82 74. Fax: 46 8 208477. E-mail: aila@polymer.kth.se.

**Table 1.** Compilation of the Cast Films

base film	film name	specification
AcGGM	G	pure, unmodified hemicellulose
70:30 AcGGM:Alg	G30A	70 wt % GGM and 30 wt % alginate
	G30A-P	plasma treatment and styrene grafting of G30A
	G30A-VP	vapor-phase grafting with styrene of G30A
	G30A-L	lamination of G30A with BnG1
70:30 AcGGM:CMC	G30C	70 wt % GGM and 30 wt % CMC
	G30C-P	plasma treatment and styrene grafting of G30C
	G30C-VP	vapor-phase grafting with styrene of G30C
benzylated GGM <sup>a</sup> (BnGGM)	BnG1	20 mL of 40 wt % NaOH, 10 g of BnCl
	BnG2	10 mL of 40 wt % NaOH, 6.66 g of BnCl
	BnG3	10 mL of 40 wt % NaOH, 15 g of BnCl
	BnG30A	benzylation of 70:30 AcGGM:Alg mixture
		10 mL of 40 wt % NaOH, 6.66 g of BnCl
	BnG5	20 mL of 13 wt % NaOH, 7.5 g of BnCl
	BnG6	20 mL of 7 wt % NaOH, 7.5 g of BnCl

<sup>a</sup> The specified amounts were added to 1.5 g of AcGGM dissolved in 50 mL of water. A 100 mg amount of TBAI (PCT) was used in all syntheses performed.

membranes. It has been shown that hydrophilic membranes are preferable,<sup>13</sup> and here membranes with a cutoff of 1000 g mol<sup>-1</sup> have been used. Hence, small molecules (i.e., salts, monomers, and oligomers <1000 g mol<sup>-1</sup>) were removed in the process. The AcGGM was concentrated from about 1 wt % to 15–20 wt %. The material used for the benzylation experiments was moreover diafiltrated after ultrafiltration in order to further purify the preconcentrate from low molecular weight substances. This was not expected to affect the composition of the hemicellulose.

Finally, the concentrates were deeply frozen using liquid nitrogen and lyophilized at -57 °C and <0.05 mbar into fluffy powder cakes. The purity of the materials was about 90%, and among the impurities lignin was the most abundant one. Further information regarding the hemicellulose isolate<sup>8</sup> as well as other similar materials<sup>16</sup> has been published earlier.

**2.2. Chemicals.** Alginic acid sodium salt from brown algae (Fluka, Germany,  $M_w = 100\,000\text{--}200\,000$  g mol<sup>-1</sup>) and carboxymethyl cellulose sodium salt, CMC, (Fluka, Germany,  $M_w = 100\,000\text{--}150\,000$  g mol<sup>-1</sup>) were used for the AcGGM blend films. Magnesium nitrate hexahydrate (>97%; Riedel-de-Haën, Germany) was used as conditioning salt. Benzophenone (BPO, 99+%; Acros, Belgium) was employed as photoinitiator in vapor-phase grafting. Styrene (≥99%; Fluka, Germany) was used as grafting agent. Benzyl chloride (BnCl, 99%; Aldrich, Germany), sodium hydroxide pellets (97–98%; Eka Nobel, Sweden), tetrabutylammonium iodide (TBAI, >99%; Sigma, Germany), and diethyl ether (Prolabo, Belgium) were used for benzylation reactions. Deuterium oxide (99.9 at. %; Aldrich, Milwaukee, WI) and deuterated dimethyl sulfoxide (DMSO-*d*<sub>6</sub>; Chemtronica, U.K.) were used for NMR analyses. Ethyl acetate (≥99%; Lab-Scan, Sweden) was used for washing after plasma treatment.

**2.3. Benzylation.** Benzylation of AcGGM was carried out in water phase in a fashion similar to that reported for other comparable polysaccharides.<sup>9–12</sup> First, 1.5 g of AcGGM formed a solution in a two-necked round-bottom flask together with 50 mL of deionized water. Then 100 mg of TBAI, acting as a phase-transfer agent (PCT), was added. Sodium hydroxide was used in various concentrations in order to observe how much base was required for activation of the hydroxyl groups. The solution temperature was kept at 40 °C for 2 h and was then raised to 100 °C. A deacetylation of the AcGGM was also caused by the base treatment. After the activation step, benzyl chloride was slowly added (see Table 1) via an attached dropping funnel under vigorous magnetic stirring. The hydrophobically modified GGM was formed as a yellowish precipitate, and the reaction was finally quenched by neutralizing (pH ~ 7) with hydrochloric acid. The benzylated product was filtered and washed subsequently several times with water and diethyl ether. Finally, the benzylated product was dried in a vacuum at

room temperature. A benzylation of a blend of 70 wt % AcGGM and 30 wt % alginate was also performed.

**2.4. Casting of Films.** The benzylated films were cast from solutions of 0.2 g of benzylated AcGGM in 2.5 mL of DMF. These were poured into glass Petri dishes (diameter, 5 cm), and the films were then left to dry in a closed hood (~23 °C, relative humidity (RH) < 50%) for 2 days. Finally, the films were conditioned in a desiccator over magnesium nitrate hexahydrate for a minimum of 48 h prior to analysis. The desiccator conditions were 51 ± 3% RH and 21 ± 1 °C.

Those films intended for lamination and surface reactions (G30A and G30C) were cast from 7 mL aqueous solutions. The selection of alginate and CMC originates from earlier positive results.<sup>8</sup> Films of pure AcGGM isolate were also cast and tested in comparison. First, hemicellulose was weighed (70 wt % of the total 0.2 g) into an Erlenmeyer flask and then mixed with alginate or CMC and heated in an oil bath at 95 °C for 20 min under magnetic stirring. The AcGGM isolate dissolved rapidly in cold water, but heating ensured a complete mixing of the components.

An overview of the films produced and investigated is shown in Table 1, where the two methods of grafting were employed according to methods developed earlier in our laboratory.<sup>15–18</sup>

**2.5. Plasma Surface Treatment.** Plasma treatment leads to reactions between the film surface and reactive species in the plasma. This introduces new functional groups at the surface, and internal surface reactions may further lead to cross-links. The gas is typically oxygen, argon, nitrogen, air, or some other gas that is not able to deposit a layer from the reacted gas at the surface. In this case argon ≥99.996% was used. Plasma treatments were then carried out in a 2.5 GHz V15-G microwave plasma system from Plasma-Finish GmbH (Germany) in argon (80 mL/min) at 300 W for 60 s at a pressure of 3 Pa.<sup>18</sup> After plasma treatment, the samples were left to stand in air in order for peroxy radicals to form. These activated radicals were then reacted by exposing samples to styrene for 15 min at room temperature. The samples were then dried, washed in ethyl acetate for 2 h, and then finally dried again at room conditions.

**2.6. Vapor-Phase Grafting.** Grafting was performed in a glass reactor consisting of two interconnected cylindrical compartments.<sup>15,17</sup> The films were placed on top of a perforated Teflon surface in one of the compartments, and this compartment was then covered with a quartz plate transparent to UV radiation. Styrene was poured into the other compartment of the reactor which was connected to a manifold. The reactor was then evacuated and slowly filled with nitrogen gas three times. Finally, the reactor chamber was evacuated, sealed, disconnected from the manifold, and submerged in a water bath (40 °C). The reactor was irradiated with UV light from an Osram Ultra-Vitalux 300 W lamp for 30 min. The reactor was placed so that a water pillar formed between

the reactor and the lamp. This ensured a stable temperature within the reactor as the water pillar absorbed heat from the UV lamp.

**2.7. Lamination.** Lamination of the film G30A was done with the benzylated AcGGM material BnG1. The film was soaked three times in a saturated solution of BnG1 in DMF. The film was air-dried between each round of lamination. The laminated film is designated G30A-L.

**2.8. Characterization.** Nuclear magnetic resonance ( $^1\text{H}$  NMR) was examined using a 400 MHz Bruker Avance instrument. Water suppression was applied. The samples were completely dissolved in  $\text{DMSO}-d_6$  before analysis.

Matrix-assisted laser desorption/ionization time-of-flight (MALDI-TOF) analyses were performed with a Bruker Ultraflex MALDI-TOF mass spectrometer with a SCOUT-MTP ion source (Bruker Daltonics, Bremen) equipped with a  $\text{N}_2$  laser (337 nm), a gridless ion source, and reflector design. A droplet of 0.3–0.5  $\mu\text{L}$  of a mixture of 20  $\mu\text{L}$  of DHB (10 mg/mL  $\text{DMSO}$ ) and 5  $\mu\text{L}$  of sample (1–2.5 mg/mL  $\text{DMSO}$ ) was placed onto a steel coordinate plate. The acceleration and reflector voltages were set to 25 and 26.6 kV, respectively, and the detector mass range was adjusted to 600–2500 kDa. The positive-ion spectra collected represented the sum of 500 laser shots, and subsequent data analysis was done with FlexAnalysis software (Bruker Daltonics).

Fourier transform infrared spectroscopy (FTIR) was employed with a Perkin-Elmer Spectrum 2000 FTIR equipped with an attenuated total reflectance (ATR) crystal accessory (Golden Gate) providing an analysis of the surface down to a depth of approximately 1  $\mu\text{m}$ . Each spectrum represented the mean of 16 scans at 2  $\text{cm}^{-1}$  resolution and was corrected for the atmospheric background. The background spectrum (empty Golden Gate unit) was recorded using the same method as that for the subsequent samples.

Differential scanning calorimetry measurements were made with a Mettler Toledo DSC 820 using a method where the sample was heated in an inert atmosphere from 30 to 280  $^\circ\text{C}$  at a rate of 10  $^\circ\text{C}/\text{min}$  in an aluminum crucible (40  $\mu\text{L}$ ) possessing a hole in the lid. The nitrogen flow was set to 50 mL/min.

The static contact angles of the film surfaces were measured using a KSV Instruments CAM200 optical contact angle and surface tension meter. The volume of the water droplets released onto the film surfaces was 6  $\mu\text{L}$ , and still pictures were taken after 5 s. The contact angle data are averages of a total of four individual measurements from two different locations on the film surface. Measurements were stopped after 10 min due to the evaporation of the water droplet.

Moisture-scan dynamic mechanical analysis was carried out on a Perkin-Elmer DMA 7 equipped with a custom-made cooling aggregate (an instrument developed and owned by STFI-Packforsk AB). Films were kept in a desiccator for a minimum of 48 h under conditions similar to those used prior to oxygen permeability measurements. Samples with a width of 3–5 mm and a height of 8–12 mm were cut for the dynamic mechanical testing. The dimensions of each sample were carefully measured, and the values were inserted into the instrument software as the mean of 10 measurement points per sample. For the measurement of storage modulus, the amplitude was varied between 2 and 6  $\mu\text{m}$  with a frequency of 1 Hz. The static forces required varied between 55 and 190 mN. The relative humidity was controlled in the measurement chamber. One scan of two samples from each film was performed. The film sample was conditioned at 20% RH for 2 h, after which a ramp up to 80% RH was applied during the DMA measurement at a rate of 1% RH/min.

The oxygen transmission of the films was measured using a Mocon Ox-Tran 2/20 apparatus (Modern Controls Inc., Minneapolis, MN) with a coulometric sensor in accordance with ASTM method D 3985-95. The area of measurement was 5  $\text{cm}^2$ , and the analyses were made at 50% RH and in case of the benzylated materials also at 83% RH. The room in which the instrument was kept had a humidity of  $50.0 \pm 6.2\%$  RH and a temperature of  $22.6 \pm 1.1$   $^\circ\text{C}$  with an oxygen flow of 20 mL/min. The permeability coefficient was calculated on the basis of the transmission and the measured thickness of the films and is presented as the average of two measurements presented as  $\text{cm}^3 \mu\text{m}/$

**Scheme 2.** Theoretical Reaction in Which AcGGM Is Fully Benzylated Exemplified by an Acetylated Mannose Unit

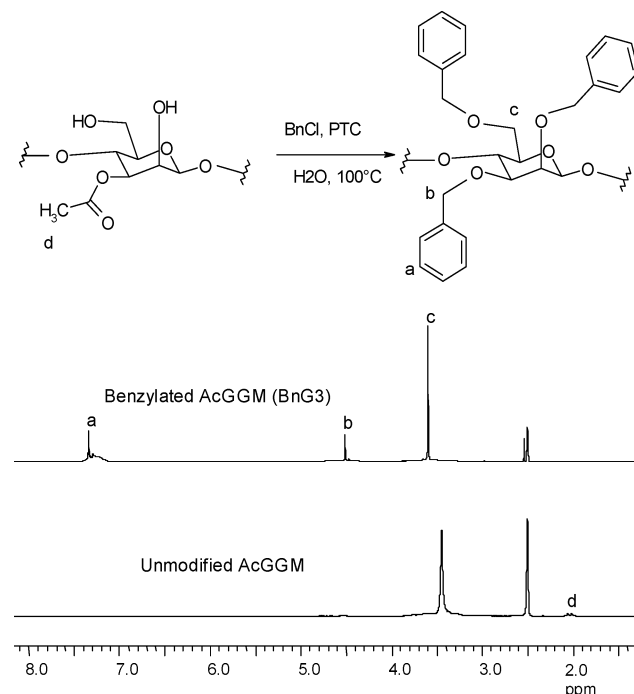


**Figure 1.** 400 MHz  $^1\text{H}$  NMR of unmodified (lower spectrum) and benzylated (BnG3) AcGGM. See Table 1 for a closer description of the BnG3 sample.

( $\text{m}^2 \text{d kPa}$ ), where 1 d = 24 h. The thicknesses of the films were measured with a micrometer (Mitutoyo) at five different locations and inserted as mean values into the computer software. The films were conditioned again for 2 h in the instrument itself before the actual measurement began. The minimum amount of time needed for the AcGGM films to stabilize at 50% and 80% RH has been ascertained by dynamic vapor sorption (DVS).

### 3. Results and Discussion

**3.1. Benzylation of Galactoglucomannan and Film Casting.** To achieve a hydrophobic modification of a galactoglucomannan isolate (AcGGM), a benzylation was performed. The reaction was performed in water phase using a phase-transfer catalyst due to the poor compatibility between the benzyl chloride and the hydrophilic polysaccharide. For activation, strong alkaline conditions are employed, which also leads to a deacetylation; see Scheme 2.

Nuclear magnetic resonance analyses show the main peaks in benzylated GGM (the upper spectrum in Figure 1) at 7.35 ppm (H of phenyl), 4.53 ppm (O- $\text{CH}_2$ -Ph), and 3.35 ppm (O- $\text{CH}_2$ -sugar). The lower spectrum in Figure 1 represents native AcGGM and is lacking the signal at 7.35 and 4.53 ppm but has instead a signal at 2.0 ppm that represents the hydrogens in the acetyl groups. This clearly indicates that substitution has taken place. Water interacts with the signal at 3.35 ppm and therefore makes the determination of an exact degree of substitution (DS) solely by NMR hard.

By using MALDI-TOF-MS, whole series of substituted GGM fragments with satisfactory intensities were observed up to a size of eight units (DP8). In Figure 2, one can see an approximately normally distributed series of the peaks representing five sugar units with benzylation. Substitution of molecular weight fragments over DP10 could not be observed, probably because of discrimination factors due to the high

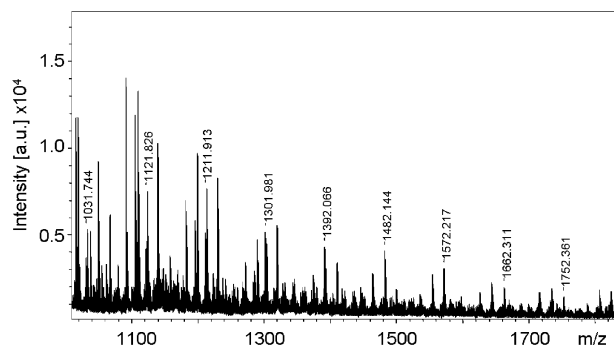


**Figure 2.** Segment of a MALDI-TOF spectrum showing the DP5 mass series of sample BnG3 mixed with a DHB matrix in DMSO.

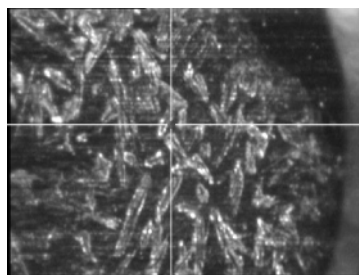


**Figure 3.** Crystal of BnG3 and DHB for MALDI.

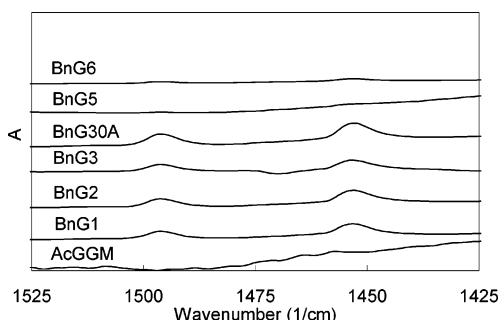


**Figure 4.** ATR-FTIR of benzylated samples (powder) between 1425 and 1525  $\text{cm}^{-1}$ .

polydispersity of the benzylated AcGGM sample.<sup>19</sup> Some segregation of the sample droplet appeared due to the low volatility of DMSO (Figure 3). However, from the MALDI-TOF-MS spectrum a DS of approximately 1.3 over the range from DP3 to DP8 could be determined.

The benzylated materials were further characterized with ATR-FTIR, and in Figure 4 the aromatic region of the spectra is shown. The vibrations of the aromatic ring can be seen most prominently by the double absorption band at  $\sim 1450$  and  $\sim 1500$   $\text{cm}^{-1}$  (Table 2). As can be noticed, the relative peak areas at 1450 and 1500  $\text{cm}^{-1}$  were not measurable for sample BnG6, indicating that the amount of base used in this specific synthesis was not sufficient to activate the hydroxyl groups of AcGGM. For the other samples, where higher concentrations of base were used, distinct aromatic peaks were observed, and the AcGGM has thus reacted with the benzyl chloride. The total area under the two peaks for each benzylation sample was found to increase with the amount of benzyl chloride added. In Table 2, the relative peak areas at 1500 and 1450  $\text{cm}^{-1}$  are presented. From the table it can be noted that BnG3 showed a lower benzylation degree than BnG2 although the charge of BnCl was higher. The large excess of benzyl chloride rendered the reaction mixture acidic and not basic in the end as in the other benzylations. The excess benzyl chloride had thus reacted with water after hydroxyl groups on the AcGGM had been consumed. The high

**Table 2.** Relative Areas of the Aromatic Ring Absorption Bands in the Range 600–2400  $\text{cm}^{-1}$  <sup>a</sup>

sample	area (1500 $\text{cm}^{-1}$ )	area (1450 $\text{cm}^{-1}$ )
G	—	—
G30A	—	—
G30A-P	0.30	0.79
G30A-VP	0.32	0.99
G30A-L	1.22	1.61
G30C	0.21	0.56
G30C-P	0.30	0.98
G30C-VP	0.21	1.10
BnG1	1.17	1.91
BnG2	1.15	1.87
BnG3	0.86	1.22
BnG30A	1.02	1.92
BnG5	0.90	1.26
BnG6	—	—

**Table 3.** Solubility of BnGGM Powder<sup>a</sup>

solvent	dielectric constant	cold	warm
cyclohexane	2	—	—
1,4-dioxane	2	xo	xo
limonene	2	—	—
diethyl ether	4	—	—
chloroform	5	—	—
ethyl acetate	6	—	—
THF	8	—	—
dichloromethane	9	—	—
pyridine	13	x	x
acetone	21	—	—
methanol	33	—	—
DMF	38	x	x
DMSO	47	x	x
water	80	—	—

<sup>a</sup> x, soluble; xo, partially soluble; —, insoluble.

temperature in combination with the acidic end pH most probably resulted in partial cleavage toward the end of the reaction of the formed ether bonds, yielding benzyl alcohol and a free hydroxyl group again. This actually opens interesting possibilities for controlling the degree of substitution at low levels since it can be expected that the distribution of benzyl groups will be very even.

Solubility (Table 3) was tested for the benzylated powders, and it was found that the benzylated materials were totally soluble in DMF, DMSO, and pyridine and partially soluble in 1,4-dioxane.

Films of the benzylated GGM were successfully cast from DMF. The transparent films showed flexibility and strength and were thus easy to handle. Due to modification, these films were more permeable to oxygen at lower humidities but were, on the other hand, less affected by the moisture at higher humidities (Table 4). We reasoned that the oxygen permeability could be lowered by a combination of unmodified and benzylated material at the same time as good water tolerance would be retained. Three different approaches were used: plasma treatment followed by styrene addition, vapor-phase grafting of styrene, and lamination with benzylated AcGGM.

**3.2. Surface Modifications and BnGGM Lamination of AcGGM Films.** For the analysis of the different surface modifications performed ATR-FTIR is well-suited since the penetration depth is limited to a few micrometers. In Figure 5, one can see that the benzyl-laminated material exhibits the largest relative absorption peak area in the aromatic region

**Table 4.** Oxygen Permeability Coefficients<sup>a</sup>

film	oxygen permeability coeff [(cm <sup>3</sup> μm)/(m <sup>2</sup> (24 h) kPa)]	
	50% RH	83% RH
G30A	0.55 ± 0.06	N/O
G30C	1.28 ± 0.15	N/O
G30C-VP	1.75 ± 0.54	N/O
G30A-L	N/A	8 ± 2 <sup>b</sup>
BnG1	559 ± 4	546 ± 2
BnG3	130 ± 2	170 ± 1
BnG5	N/A	153 ± 4

<sup>a</sup> N/A, not analyzed; N/O, not obtained. <sup>b</sup> At 73% RH.

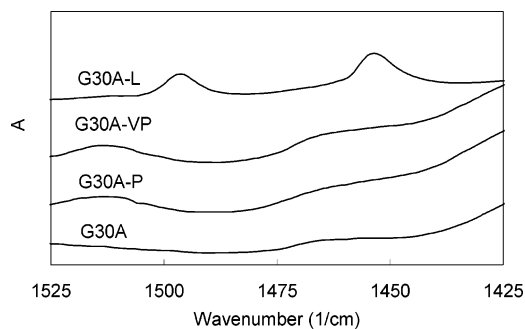


**Figure 5.** Segment of FTIR of the films G30A (no posttreatment), G30A-P (plasma treated and grafted with styrene), G30A-VP (vapor-phase grafted with styrene), and G30A-L (laminated with BnG1).

**Table 5.** Glass Transition and Degradation Temperatures for BnGGM

sample	$T_g$ (°C)	onset temp of degradation (°C)
G	~60 (second scan)	~220
BnG1		~250
BnG2		~250
BnG3	~105 (second scan)	~260
BnG30A	~130 (first scan)	~230
BnG5	~60 (first scan)	<200
BnG6	~60 (first scan)	<200

among the modifications of G30A. The plasma-treated and styrene-grafted G30A-P and the styrene vapor-phase grafted G30A-VP both demonstrated slightly lower absorption than the benzyl-laminated G30A-L, but substantially higher absorption than the unmodified film G30A, indicating that grafting has occurred. The area under the aromatic peak region for G30A-VP was bigger than that for G30A-P; i.e., more styrene molecules were able to attach to the UV-irradiated film. Lamination clearly resulted in a thicker layer of styrene molecules on the AcGGM surface than the two grafting methods.

**3.3. Material and Film Properties.** Differential scanning calorimetry (DSC) resulted in the elucidation of a  $T_g$  for some of the benzylated materials (Table 5 and Figure 6). For native AcGGM the discontinuity in the temperature range of 55–65 °C represents a glass transition.<sup>10</sup> A difficulty in the determination of the  $T_g$  is the overlapping peak resulting from the large amount of hydroxyl groups causing hydrogen bonds in the polysaccharide. The benzylated material BnG3 lacks this overlapping peak since the hydrogen bonding capability is strongly reduced. A discontinuity in the baseline at around 105 °C shows the  $T_g$ , which in other words is higher than for the unmodified material. This value is also in accordance with what has earlier been reported for konjac glucomannan.<sup>9</sup> Samples

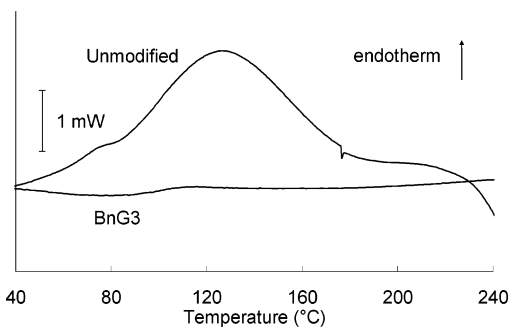


**Figure 6.** Glass transition of benzylated and native AcGGM (second scans of same sample).

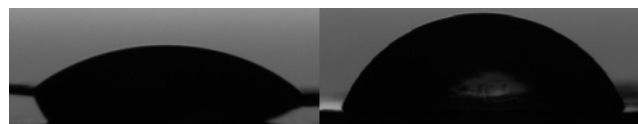


**Figure 7.** Water droplets (6 μL) on unmodified AcGGM (left) and BnG2 (right) after 50 s.

**Table 6.** Static Contact Angle Measurements after 5 s and the Adsorption Time of the Water Droplet

sample	contact angle (deg)	adsorption time
G	63 ± 3	50–60 s
G30A	78 ± 3	80–100 s
G30A-P	75 ± 1	170–190 s
G30A-VP	71 ± 2	150–170 s
G30A-L	63 ± 2	> 10 min
G30C	54 ± 3	20–25 s
G30C-P	72 ± 4	115–125 s
G30C-VP	72 ± 3	85–95 s
BnG1	57 ± 4	> 10 min
BnG2	68 ± 3	> 10 min
BnG3	70 ± 2	> 10 min
BnG30A	45 ± 7	> 10 min
BnG5	68 ± 7	> 10 min

BnG5 and BnG6 had a lower DS than the other materials, and thus their  $T_g$  is in the range of the unmodified AcGGM. Distinct glass transition temperatures were, for unknown reasons, not found for materials BnG1 and BnG2. Since the DSC results showed a second scan  $T_g$  for BnG3, this indicates thermoplastic behavior and that it might be possible to extrude the benzylated GGM.

It is expected that the hydrophobic modifications should affect the contact angle and/or the adsorption of a water droplet. Contact angles depend on two main characteristics: polarity and surface roughness. When measuring static contact angles with water, nonpolar surfaces result in higher angles due to forces of repulsion. As can be seen from Table 6, the contact angles obtained for the film samples were found to be quite similar to each other. The surprisingly high contact angle of the unmodified AcGGM film could be explained by the distribution of, e.g., lignin remnants onto the film surface.

The adsorption behavior of the materials varied greatly. The benzylated samples did not adsorb the water droplet for as long as we measured (10 min) even though they did not exhibit the highest contact angles. In Figure 7, a contact angle measurement of an unmodified and a benzylated film sample (BnG2) is shown. After 50 s, the unmodified film sample had partially adsorbed the water droplet, while the contact angle of the droplet on the benzylated film did not change at all as mentioned.

The plasma-treated films all adsorbed the water droplet fairly quickly probably due to the drying of the film in a vacuum

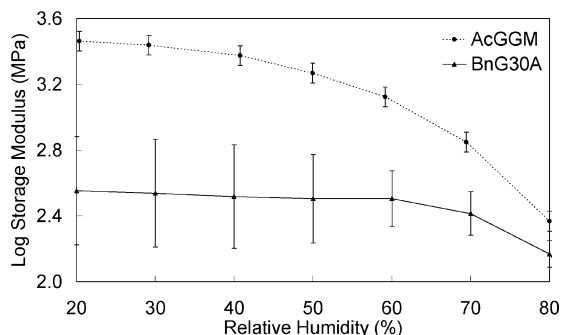


**Figure 8.** Comparison of DMA measurements for AcGGM and BnG30A.

**Table 7.** Water Solubility of Chosen Benzylation Samples

film	weight left (%)		
	7 days	19 days	26 days
BnG1	74	74	72
BnG3	88	86	84
BnG30A	83	79	77

during plasma treatment. The benzyl-laminated G30A films repelled the water droplet for as long as the benzylated films. Regarding the benzylated materials, the low contact angle for the BnG30A film could be related to more free carboxyl groups. The lack of hydrogen bonds in the BnGGM films is also evident from DSC measurement (see Figure 6).

In Table 7, the water solubility was tested by immersing the film samples in water and measuring the weight loss. The weight losses of BnG1, BnG3, and BnG30A were in the range 16–28 wt % but seemed constant over time. It is likely that some less reacted material dissolved and caused the weight decrease.

The water solubilities of film samples G30A, G30A-P, and G30A-VP were also tested, but all of them dissolved almost immediately after addition of water. The fact that the benzylated samples did not dissolve showed a distinct difference between film surface and bulk modification. The laminated film sample was less soluble than the unmodified films, as expected, but still more soluble than the bulk modified films (dissolution occurred mainly from the cut film edges). As a rule of thumb, the unmodified, VP-grafted, and plasma-treated films dissolved in minutes, the laminated in hours, and the bulk modified films probably in months, or even years.

**3.4. Moisture Tolerance and Oxygen Permeability.** The influence of water vapor on the mechanical properties of the film can be effectively studied by moisture-scan dynamic mechanical analysis (DMA). This technique is also interesting from the perspective that it is expected to relate to the barrier properties. Moisture-scan DMA was carried out on a fragile unmodified AcGGM film sample and a benzylated film sample, BnG30A. Figure 8 clearly shows that the unmodified sample dampens at lower humidity than the benzylated sample. This is simply explained by the attachment of hydrophobic side groups. With these measurements as a basis, we could predict that the oxygen permeability of the benzylated films would be relatively stable over increasing humidity. The time period between 60% and 80% RH is only 20 min, and it is expected that the difference observed in the storage modulus in Figure 8 would be larger if the rate was slower than 1%/min.

In Table 4, the oxygen permeability coefficients of unmodified AcGGM blend films, benzylated GGM films, and the laminate film can be found. Due to less hydroxyl functions on the benzylated GGM, permeability at 50% RH dropped com-

pared to the unmodified material. However, the values are comparable to more traditional packaging materials used today like polyethylene (PE) and ethylene vinyl acetate (EVA). LDPE has an oxygen permeability coefficient of 102–188 and EVA 177–263 ( $\text{cm}^3 \mu\text{m})/(\text{m}^2 (24 \text{ h}) \text{kPa})$  for 25  $\mu\text{m}$  thick films at 50% RH.<sup>20</sup> We obtained permeability measurements at 83% RH for films of benzylated materials which could not even be achieved for the unmodified blend films due to their elevated moisture sensitivity. The moisture sensitivity of the unmodified material is also demonstrated in Figure 8, where the dynamic mechanical response as a function of humidity is displayed.

BnG3 and BnG5 exhibit better values than BnG1 at elevated humidity. BnG1, on the other hand, showed more stable results over varying humidity content. This is logical since the degree of substitution was less for BnG3 and BnG5 than for BnG1 according to FTIR analyses. The low fluctuation in oxygen permeability between 50% and 83% RH for the benzylated samples is supported by the DMA measurements where the benzylated material showed more mechanical stability over varying relative humidity than an unmodified sample (Figure 8). By the combined approach using lamination of a AcGGM–alginate blend film with benzylated GGM, excellent barrier properties were recorded ( $8 \text{ cm}^3 \mu\text{m m}^{-2} (24 \text{ h}^{-1}) \text{kPa}^{-1}$  at 83% RH).

#### 4. Conclusion

In this paper, benzyl galactoglucomannan (BnGGM) was produced and subsequently used to manufacture flexible and transparent water-resistant films. The oxygen permeability was evaluated, and it was found that the films possessed oxygen barrier properties that are less sensitive to moisture than unmodified acetylated galactoglucomannan. To achieve a combination of both moisture tolerance and high barrier properties, three different strategies were then tested utilizing unmodified acetylated galactoglucomannan as the base material for the films. Plasma treatment followed by styrene addition (i), vapor-phase grafting of styrene (ii), and lamination with a benzylated polysaccharide (iii). The vapor-phase-grafted films show better tolerance toward humidity than the plasma-treated ones. A well-adhering unique laminate employing a modified and an unmodified hemicellulose could be manufactured and gave efficient water protection on the basis of contact angle measurements. It is likely that normal extrusion equipment could be used for the purpose of lamination. The lamination thus seemed to be a promising route for obtaining good barrier properties even at higher humidities.

**Acknowledgment.** At STFI-Packforsk AB we thank Associate Prof. Olof Dahlman and Dr. Anna Jacobs for the concentration by ultrafiltration and characterization carried out on the hemicellulose, as well as Associate Prof. Lennart Salmén and Anne-Mari Olsson for the use of the DMA instrument and their expertise on the subject. Professor Guido Zacchi and M.Sc. Tobias Persson are thanked for the concentration by microfiltration, ultrafiltration, and diafiltration of AcGGM at the Department of Chemical Engineering, Lund University, Sweden. Stora Enso is thanked for providing the raw material. Financial support from the Swedish Agency for Innovation Systems (VINNOVA) within the program of green materials “Gröna Material” is gratefully acknowledged.

#### References and Notes

- (1) Leuchs, O.; Dorr, E. (I. G. Farbenindustrie AG). DE 00000554309A, 1932.

- (2) Hon, D. N. S.; Ou, N. H. *J. Polym. Sci., Part A: Polym. Chem.* **1989**, *27*, 2457–2482.
- (3) Hon, D. N. S.; Chao, W. Y. *J. Appl. Polym. Sci.* **1993**, *50*, 7–11.
- (4) Joaquim, A. P.; Curvelo, A. A. S.; Botaro, V. R.; Carvalho, A. J. F.; Gandini, A. *Cellul. Chem. Technol.* **2003**, *36*, 459–470.
- (5) Zemke, G. W.; Moro, J. R.; Gomez-Pineda, E. A.; Winkler-Hechenleitner, A. A. *Int. J. Polym. Mater.* **1996**, *34*, 197–210.
- (6) Bowry, S. K.; Rintelen, T. H. *ASAIO J.* **1998**, *44*, M579–M583.
- (7) Timell, T. E. *Wood Sci. Technol.* **1967**, *1*, 53.
- (8) Hartman, J.; Albertsson, A.-C.; Söderqvist Lindblad, M.; Sjöberg, J. *J. Appl. Polym. Sci.*, in press.
- (9) Lu, Y.; Zhang, L. *Polymer* **2002**, *43*, 3979–3986.
- (10) Chen, Y.; Zhang, L.; Lu, Y.; Ye, C.; Du, L. *J. Appl. Polym. Sci.* **2003**, *90*, 3790–3796.
- (11) Ebringerova, A.; Novotna, Z.; Kacurakova, M.; Machova, E. *J. Appl. Polym. Sci.* **1996**, *62*, 1043–1047.
- (12) Vincendon, M. *J. Appl. Polym. Sci.* **1998**, *67*, 455–460.
- (13) Persson, T.; Jönsson, A.-S.; Zacchi, G. 14th European Biomass Conference and Exhibition, 2005.
- (14) Jacobs, A.; Lundqvist, J.; Stålbrand, H.; Tjerneld, F.; Dahlman, O. *Carbohydr. Res.* **2002**, *337*, 711–717.
- (15) Ranby, B. *Polym. Eng. Sci.* **1998**, *38*, 1229–1243.
- (16) Wirsen, A.; Sun, H.; Albertsson, A.-C. *Biomacromolecules* **2005**, *6*, 2697–2702.
- (17) Edlund, U.; Kaellrot, M.; Albertsson, A.-C. *J. Am. Chem. Soc.* **2005**, *127*, 8865–8871.
- (18) Olander, B.; Wirsen, A.; Albertsson, A.-C. *Biomacromolecules* **2002**, *3*, 505–510.
- (19) Jacobs, A.; Dahlman, O. *Biomacromolecules* **2001**, *2*, 894–905.
- (20) Massey, L., Ed. *A Guide to Packaging and Barrier Materials. Permeability Properties of Plastics and Elastomers*, 2nd ed.; William Andrew Inc.: Norwich, NY, 2003.

BM060129M